

Compaction of Anisotropic Granular Materials: Symmetry Effects

Lj. Budinski-Petković¹, M. Petković², Z.M. Jakšić³ and S.B. Vrhovac^{3,a}

¹Faculty of Engineering, Trg D. Obradovića 6, Novi Sad 21000, Serbia and Montenegro

²DMS group, Puškinova 9A, Novi Sad 21000, Serbia and Montenegro

³Institute of Physics, P.O. Box 68, Zemun 11080, Belgrade, Serbia and Montenegro

^avrhovac@phy.bg.ac.yu

Keywords: Granular Compaction, Granular Materials, Lattice Model.

Abstract. We perform numerical simulation of a lattice model for the compaction of a granular material based on the idea of reversible random sequential adsorption. Reversible random sequential adsorption of objects of various shapes on a two-dimensional triangular lattice is studied numerically by means of Monte Carlo simulations. The growth of the coverage $\rho(t)$ above the jamming limit to its steady-state value ρ_∞ is described by a pattern $\rho(t) = \rho_\infty - \Delta\rho E_\beta[-(t/\tau)^\beta]$, where E_β denotes the Mittag-Leffler function of order $\beta \in (0, 1)$. For the first time, the parameter τ is found to decay with the desorption probability P_- according to a power law $\tau = A P_-^{-\gamma}$. Exponent γ is the same for all shapes, $\gamma = 1.29 \pm 0.01$, but parameter A depends only on the order of symmetry axis of the shape. Finally, we present the possible relevance of the model to the compaction of granular objects of various shapes.

Introduction

A large variety of physical, chemical and biological processes can be modeled by random sequential adsorption (RSA) on a lattice [1]. In this process particles are adsorbed, one at a time, at randomly chosen sites of a d-dimensional lattice, subject to constraints imposed by interaction with previously deposited particles. The adsorbed particles are permanently fixed at their spatial positions and the deposition process ceases when all unoccupied spaces are smaller than the size of an adsorbed particle. For lattice models, the asymptotic approach of the density $\rho(t)$ to its jamming limit ρ_{jam} is known to be given by exponential time dependence:

$$\rho(t) \sim \rho_{jam} - \Delta\rho \exp(-t/\sigma), \quad (1)$$

where $\Delta\rho$ and σ are parameters that depend on the shape and orientational freedom of depositing objects [1, 2].

The deposition of proteins and colloids from solution onto solid surfaces often involves alternating adsorption/desorption steps. The kinetics of the reversible RSA is governed by the ratio of adsorption/desorption rate, $K = k_+/k_-$ [3,4]. For large values of K , there is a rapid approach to density $\rho \cong \rho_{jam}$, followed by a slow relaxation to a larger steady-state value ρ_∞ . At very early times of the process, when the coverage is small, the adsorption process is dominant and the coverage grows rapidly in time; for large enough densities ($\rho > \rho_{jam}$) the compaction mechanism requires the rearrangement of the increasing number of particles in order to open a hole large enough for the insertion of an additional particle, and the role of desorption is crucial.

Understanding the kinetics of irreversible/reversible RSA of shapes other than the line segments on a 1D lattice lacks rigorous results by analytical methods and the numerical simulations remain one of the primary tools for investigating these problems. The numerical analyses for the RSA of extended objects on the triangular lattice [5] establish that the coverage $\rho(t)$ follows the exponential law (1) at long times with the rate σ dependent mostly on the order of symmetry of the shape. A number of papers [5-7] concerning irreversible or reversible RSA also confirm the crucial

role of the geometrical character of objects in RSA dynamics. In some numerical studies of RSA a power-law dependence is observed even on a discrete lattice [7,8]. To the best of our knowledge, there are no reports on *reversible* RSA of extended objects of shapes other than line segments [3, -9] on a *triangular* lattice.

Definition of the model and the simulation method

In this paper we present the results for the Monte Carlo simulations of the reversible RSA of extended objects on a triangular lattice. The depositing objects are formed by self-avoiding random walks and we concentrate on the influence of the shape on the kinetics of the adsorption-desorption process. For a small number of steps it is easy to find all the shapes that may show different time behavior of $\rho(t)$, which enables a systematic approach to this problem. We performed numerical simulations for all such shapes of length $l = 1, 2$ and 3 , covering two, three and four lattice sites, respectively. On a triangular lattice shapes with a symmetry axis of first, second, third and sixth order can be formed. The simulations are also performed for a few more objects of greater lengths, including one more object with a symmetry axis of third order and two objects with symmetry axis of sixth order. All these objects are shown in Table 1. The Monte Carlo simulations are performed on a triangular lattice of size $L = 120$. Periodic boundary conditions are used in all directions and objects are not allowed to overlap. At each Monte Carlo step, adsorption is attempted with probability $P_+ = 1$ and desorption with probability P_- . The time t is counted by the number of adsorption attempts per lattice site.

Results and Discussion

The time behavior of the density $\rho(t)$ for various objects in Table 1 is illustrated in Fig. 1, where a relatively low value of P_- has been used ($P_- = 0.0005$). We have tried to fit different functional forms to the simulation data in Fig. 1, looking in particular at the relaxation functions proposed in the experimental and numerical studies of complex systems [10]. We have found that the commonly claimed stretched exponential relaxation does not hold for many objects, especially for those with the symmetry axis of higher order ($n_s \geq 3$). Instead, the most suitable functional form for our data is a Mittag-Leffler function, which is a natural generalization of the exponential function [11]. The fitting function that we have used is:

$$\rho(t) = \rho_\infty - \Delta\rho E_\beta [-(t/\tau)^\beta], \quad \Delta\rho = \rho_\infty - \rho_0, \quad (2)$$

where ρ_∞ , ρ_0 , τ , and β are the fitting parameters. E_β denotes the Mittag-Leffler function of order β . The Mittag-Leffler function interpolates between the initial stretched exponential form $\sim \exp[-(t/\tau)^\beta/\Gamma(1+\beta)]$, $t \ll \tau$, and the long-time power-law behavior $\sim (t/\tau)^{-\beta}/\Gamma(1-\beta)$, $t \gg \tau$. This property of Mittag-Leffler function enables us to rewrite Eq. (2) as

$$\rho(t) = \rho_\infty - \Delta\rho \exp[-(t/\tau)^\beta/\Gamma(1+\beta)], \quad t \ll \tau, \quad (3)$$

$$\rho(t) = \rho_\infty - \Delta\rho (t/\tau)^{-\beta}/\Gamma(1-\beta), \quad t \gg \tau. \quad (4)$$

















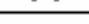





The solid lines through the data in Fig. 1 are fits to Eq. (2). All fits have been performed for $\rho(t) \geq \rho_{jam}$. As it can be seen, the intermediate-long time behavior can be accurately fitted by the Mittag-Leffler function (2). The fitting parameters τ and β are given in Table 1 for two values of desorption probability: $P_- = 0.0005, 0.001$. The parameter ρ_∞ is the equilibrium value of $\rho(t)$ when $t \rightarrow \infty$, and $\rho_0 \approx \rho_{jam}$. The accurate estimates for the jamming coverages ρ_{jam} can be found in [5].

According to τ , all shapes from Table 1 can be divided into four groups. In particular, when $P_- = 0.0005$ we distinguish: (i) shapes with a symmetry axis of first order, $n_s = 1$, with $\tau \leq 764$; (ii) shapes with a symmetry axis of second order, $n_s = 2$, with $\tau \in [807 - 1198]$; (iii) shapes with a symmetry axis of third order, $n_s = 3$, with $\tau \in [833 - 1500]$; and (iv) shapes with a symmetry axis of

sixth order, $n_s = 6$, with $\tau \geq 1550$. We notice that the time τ physically signals the crossover from a stretched exponential scaling (3) to a power law behavior (4). If only $\beta \neq 1$, the relaxation has an algebraic decay. The shapes of higher order of symmetry n_s have higher values of τ . This means that the dynamics gets drastically slower when n_s increases. The crossover time τ is also sensitive to variations of desorption probability P_- and decreases with increasing P_- for the same type of shape.

The data for k -mers (objects 1, 2, 5, 14, 15, and 19 in Table 1) suggest that the parameter τ is almost independent on the size of the shape. However, the fitting parameter β strongly depends on both the symmetry order and the size of the object. The parameter β decreases with the size and with the order of symmetry axis of the shape, which means that the evolution towards the steady-state density ρ_∞ takes place on a much wider time scale.

Table 1 Parameters τ and β determined using Eq. (2) for various shapes on a triangular lattice and for two different values of P_- . The colors (online only) are associated with the different order n_s of symmetry axis.

	shape	n_s	ℓ	$P_- = 0.0005$		$P_- = 0.001$		
				τ	β	τ	β	
(1)		2	2	895	0.823	402	0.888	
(2)		2	3	986	0.711	434	0.776	
(3)		1		675	0.822	279	0.904	
(4)		3		1500	0.785	630	0.825	
(5)		2	4	1048	0.678	431	0.732	
(6)		1		608	0.822	242	0.851	
(7)		1		583	0.853	249	0.908	
(8)		2		1198	0.676	473	0.731	
(9)		1		609	0.824	246	0.864	
(10)		1		764	0.810	307	0.862	
(11)		2		943	0.793	390	0.855	
(12)		1		597	0.859	238	0.900	
(13)		1		582	0.852	249	0.907	
(14)		2		5	985	0.684	413	0.730
(15)		2		6	922	0.683	368	0.732
(16)		3			833	0.774	346	0.822
(17)		6			1950	0.595	808	0.647
(18)		1	605	0.745	241	0.821		
(19)		2	7	807	0.681	353	0.731	
(20)		6		1550	0.567	670	0.645	
(21)		1		596	0.727	240	0.811	
(22)		1		421	0.731	190	0.825	

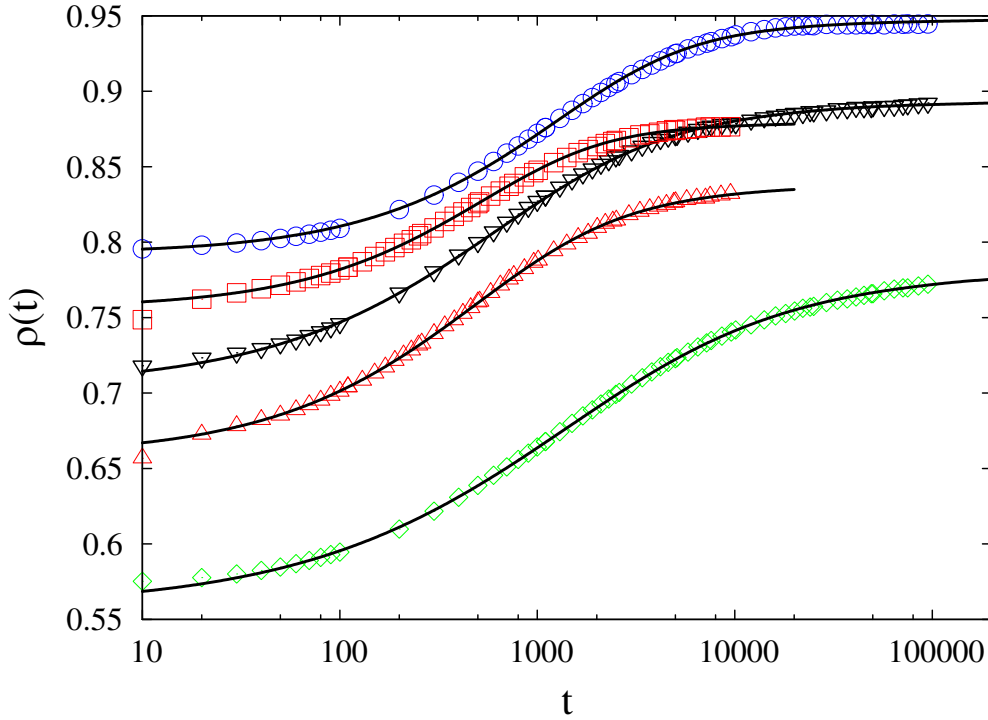


Fig. 1 (Color online) Temporal behavior of density $\rho(t)$ for desorption probability $P_- = 0.0005$ for various shapes from Table 1: 4 (O), 9 (□), 17 (◇), 18 (Δ) and 19 (▽). Continuous curves are the Mittag-Leffler fits of Eq. (2), with the parameters given in Table 1.

In order to gain a better understanding of the symmetry effects, we investigated the dependence of the fitting parameters τ and β on desorption probability P_- , in detail. The data for τ and β vs P_- for various objects are plotted in Fig. (2). The increase of β with P_- is more pronounced for objects with higher order of symmetry axis. For large values of P_- , parameter β reaches a value close to 1. Since $E_\beta[-(t/\tau)^\beta] \rightarrow \exp(-t/\tau)$ when $\beta \rightarrow 1$, the multi-stage relaxation feature disappears in the regime of strong desorption. It is remarkable that the parameter τ , for a given symmetry order, seems to be a simple power law of the desorption probability P_- :

$$\tau = A(P_-)^{-\gamma} \quad (5)$$

with the same exponent $\gamma = 1.29 \pm 0.01$ for *all* shapes.

The dependence of the fitting parameters τ and β on the desorption probability P_- is shown in Fig. 3 for the reversible deposition of k -mers ($k=2-7$). The first observation is the collapse of the τ vs P_- curves. This means that the parameter A of the power law (5) can be considered as almost independent of the size of k -mers. As seen in Figs. 2 and 3, the parameter A depends only on the order of symmetry axis of the shape. We have obtained that $A = 0.038, 0.058, 0.076, 0.083$ for $n_s = 1, 2, 3, 6$, respectively.

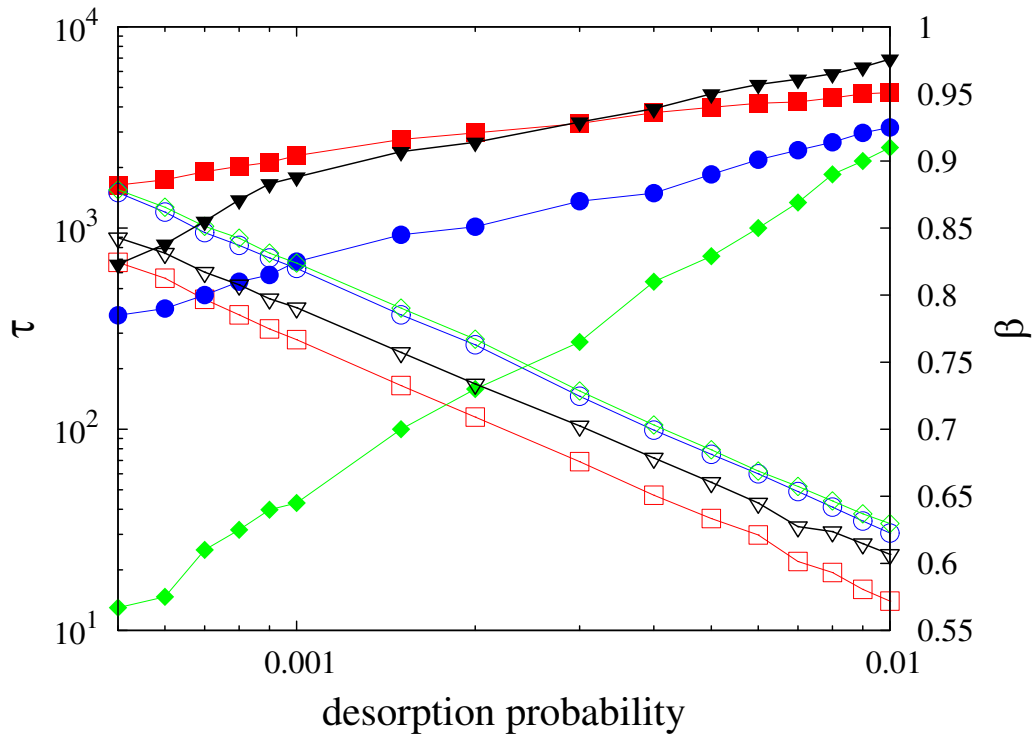


Fig. 2 (Color online) Parameters τ (empty symbols) and β (full symbols) of fit (2) vs desorption probability P_- for several shapes from Table 1. Triangles, squares, circles and diamonds correspond to shapes (1), (3), (4) and (20) in Table 1, respectively.

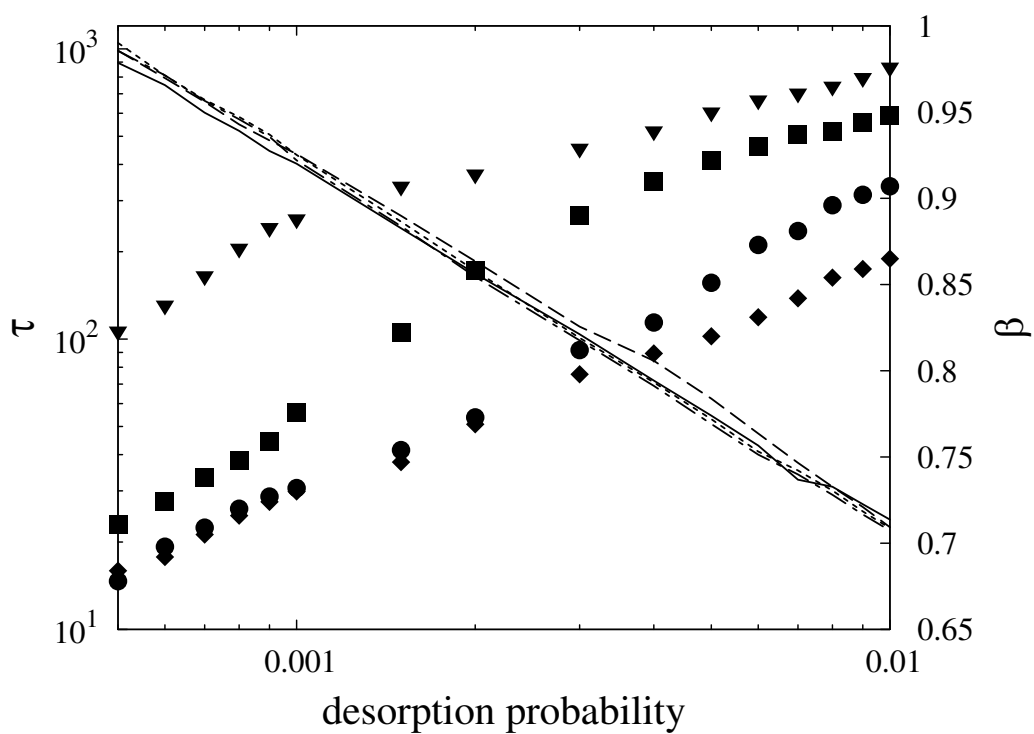


Fig. 3 Parameters τ (lines) and β (symbols) of fit (2) vs desorption probability P_- for k -mers ($k = 2, 3, 4, 5$) on the triangular lattice. Triangles, squares, circles and diamonds (or solid, dashed, dotted and dot-dashed lines) correspond to $k = 2, 3, 4, 5$, respectively.

It is now useful to explore the possible reason for slowing down of the deposition dynamics with increasing order of symmetry of the shape. When a value ρ_{jam} is reached, the rare desorption events are generally followed by immediate readsorption. The total number of particles is not changed by these *single* particle events. However, when one bad sited object desorbs and two particles adsorb in the opened good locations, then the number of particles is increased by one. Likewise, if two good-sited objects desorb and a single object adsorbs in their stead, the number of particles is decreased by one. These *collective* events are responsible for the density growth above ρ_{jam} . The symmetry properties of the shapes have a significant influence on the filling of small isolated targets on the lattice. Indeed, there is only a restricted number of possible orientations in which an object can reach a previously opened location, provided the location is small enough. For a shape with symmetry axis of higher order there is a greater number of possible orientations for deposition onto an isolated location and an enhanced probability for readsorption. Hence, the increase of the order of symmetry of the shape enhances the rate of *single* particle readsorption. This extends the mean waiting time between consecutive two-particle events and causes a slowing down of the densification.

Conclusion

We have performed extensive simulations of reversible RSA using objects of different sizes and rotational symmetries on a triangular lattice. A systematic approach is made by examining a wide variety of object shapes. The large number of examined objects represents a good basis for testing various fitting functions and finding a universal functional type that describes the time coverage behavior $\rho(t)$ in the best way. We have fitted the time dependences of the coverage fraction above the jamming limit ρ_{jam} with the Mittag-Leffler function (2). Simulation shows that the coverage kinetics strongly depends on the symmetry properties of the shapes. It has been also shown that the dynamical behavior is severely slowed down with the increase of the order of symmetry of the shape. We have also pointed out the importance of collective events for governing the time coverage behavior of shapes with different rotational symmetry.

As an open possibility for the future, we think that the two-dimensional model presented in this work can be generalized to mixtures of several kinds of objects [5]. This would allow us to study the compaction process in *polydisperse* granular systems under tapping [12].

Acknowledgement

This research has been supported by the MNTRS under Projects Nos. 1895, 1469, and 1478.

References

- [1] J. W. Evans: Rev. Mod. Phys. Vol. 65[4] (1993), p. 1281.
- [2] V. Privman: Colloids and Surfaces A Vol. 165[4] (2000), p. 231.
- [3] R.S. Ghaskadvi and M. Dennin: Phys. Rev. E Vol. 61 [2] (2000), p. 1232.
- [4] A.J. Kolan, E.R. Nowak and A.V. Tkachenko: Phys. Rev. E Vol. 59 [3] (1999), p. 3094.
- [5] Lj. Budinski-Petković and U. Kozmidis-Luburić: Phys. Rev. E Vol. 56 [6] (1997), p. 6904.
- [6] M.D. Khandkar, A.V. Limaye and S.B. Ogale: Phys. Rev. Lett. Vol. 84 [3] (2000), p. 570.
- [7] J.-S. Wang and R.B. Pandey: Phys. Rev. Lett. Vol. 77 [9] (1996), p. 1773.
- [8] J.W. Lee and B.H. Hong: J. Chem. Phys. Vol. 119 [1] (2003), p. 533.
- [9] J.W. Lee: Physica A Vol. 331 (2004), p. 531.
- [10] J.C. Phillips: Rep. Prog. Phys. Vol. 59 (1996), p. 1133.
- [11] R.K. Saxena, A.M. Mathai and H.J. Haubold: Physica A Vol. 344 (2004), p. 657.
- [12] M. Wackenhut and H. Herrmann: Phys. Rev. E Vol. 68 (2003), p. 041303.